ICAS 2016
30th Congress of the International Council of the Aeronautical Sciences
DCC, Daejeon, Korea ; September 25-30, 2016

EXPERIMENTAL AND COMPUTATIONAL STUDY OF GROUND EFFECT ON AIRFOIL SECTION

Zdeněk Pátek*, Petr Vrchota*, Jan Červinka*
***VZLU Aerospace Research and Test Establishment, Prague, Czech Republic**

Keywords: *ground effect, airfoil section, sailplane*

Abstract

The influence of ground proximity on aerodynamic characteristics of an airfoil was studied at low Reynolds number. The study, motivated mainly by sailplane take-off and landing safety, provides information about the development of the pressure distributions and of the aerodynamic forces acting on the airfoil with the approaching of the airfoil to the ground. Differences caused by fixed or by moving ground were examined using CFD computations.

Nomenclature

c	airfoil chord
C_D	drag coefficient
C_L	lift coefficient
C_L	lift coefficient at $\alpha = 0$
C_m	moment coefficient
C_p	pressure coefficient
h	height above the ground
x	longitudinal coordinate along the airfoil chord
α, AoA	angle of attack

Subscripts

MAX	maximum
MIN	minimum

1 Introduction

The ground effect is an important phenomenon known for decades, it was studied even as early as in 1920s [1]. The flowfield around an airfoil is gradually developed, to the extent depending strongly nonlinearly on distance between the airfoil and the ground. Typically presented results of both experimental and computational studies are focused on the positive effects of the ground proximity: increase of the lift coefficient and decrease of the drag coefficient at constant angle of attack, e.g. [2][3][4][5] and many others. To study the potential advantages of the phenomena, many studies were performed, focused frequently on over-water or wing-in-ground-effect vehicles, recently for example [6][7], or on race cars (for example [8][9] examining "inverted" cambered airfoil producing downward oriented lift).

2 Motivation

The aim of the study was to investigate in detail the aerodynamics of an airfoil approaching to the ground for extended range of distances and extended range of angles of attack. The reasoning for this study is initiated especially by the problems encountered during sailplane take-off where the touch of the wingtip with the ground during the take-off run is quite common. If the pilot does not manage to level the wing immediately, he should promptly abort the take-off, otherwise potentially dangerous situation would be developed. If the speed is already too high or the pilot underestimates the problem, the wingtip adhering on the ground can result in uncontrolled violent lateral or rotational movement on the ground damaging the sailplane with potentially severe consequences – many accidents are reported every year.

Recently a study dedicated to the gliders was performed [5] but aimed primarily at validation of a CFD code, analysing the increase of the lift and reduction of the drag in the

proximity of the ground and possibilities of their exploitation.

The presented study is not focused on "positive" effects only but is concentrated especially on unfavourable and dangerous phenomena that are substantial for the safety of the take-off. The combination of a wind tunnel experiment and CFD computations is used, as it seems to be the most efficient way.

3 Experimental Facility

3.1 Wind Tunnel

A wind tunnel with closed test section of rectangular cross-section of 0.45 m to 0.45 m was used for the testing. The maximum flow velocity was 40 metres per second, the velocity variation below 0.5 per cent, the angularity variation below 0.5 deg, the turbulence intensity 0.3 per cent.

The model of the airfoil section was of "from the wall to the wall" type, sufficient two-dimensionality of the flow was checked by hot-wire anemometer measurement.

3.2 Model

A model of NACA 0012 symmetric airfoil of maximum thickness of 12 per cent was used for the investigation. The model of chord of 0.100 m was equipped with 29 pressure taps of 0.4 mm diameter. The well-known symmetric airfoil was chosen as there are many experimental and computational results available for it and its maximum thickness corresponds suitably to sailplane technology. A symmetric airfoil is advantageous because it provides fair comparison of development of the flow on the upper and the lower surface respectively, without disturbances caused by different geometrical shapes of the surfaces.

The ground plane was simulated by means of a flat plate with smoothly shaped leading edge, the distance between the airfoil and the plate was adjustable.

3.3 Experimental Methods

The surface pressures were scanned through a Scanivalve system. The lift and moment coefficients were measured by means of a strain-gauge balance.

The drag was evaluated from wake measurements performed by a rake probe.

The uncertainty analysis of measured force coefficients gives ±0.01 in C_L, ±0.003 in C_D, ± 0.005 in C_m, ±0.05 in C_p.

4 Wind Tunnel Testing

The examined heights of the airfoil above the ground plane were corrected by the momentum thickness of the boundary layer of the ground plane, so the distance h is the distance between the point positioned at 0.40 of the airfoil chord and the upper boundary of the boundary layer momentum thickness of the ground plane. The boundary layer velocity profile was measured by a hot-wire anemometer. The infinite value of h/c represented the airfoil in the unrestricted space, the coefficients for this case were obtained by means of the standard low-speed wind tunnel corrections [10].

The angle of attack was changed from -6 degrees up to 2 degrees over the angle of the fully developed stall. The distance h/c = 0.15 was an exception as it was impossible to extend the angle of attack over 6 degrees due to the near proximity of the airfoil to the ground plane and its boundary layer.

Depending of the angle of attack and the distance between the airfoil surface and the ground plane, the geometrical character of the shape of the gap between the airfoil and the ground plane is changed, which seems to be an important factor at certain conditions.

The wind tunnel testing was performed at Reynolds number of $0.22 \cdot 10^6$ which well represents the sailplane wingtip at low speed.

5 CFD Computations

5.1 Grid creation

The grid was created as a multi block structured grid from hexahedral elements in ICEM CFD

program. The grid had identical parameters for all calculations (boundary layer resolution, number of the elements, ...).

5.2 Solver

A flow solver EDGE [11] for unstructured grids was used for CFD calculations. It is based on a finite volume approach with median dual grids. The solver adopted an edge-based formulation for arbitrary elements and used a node-based finite volume technique to solve governing equations. The governing equations were integrated explicitly toward steady state with Runge-Kutta time integration. The convergence was accelerated with agglomeration multigrid and implicit residual smoothing. Central spatial discretization was used for the convection of the mean flow and a second-order upwind scheme was used for the turbulence, in which the second order was enforced by a total-variation-diminishing limiter. Compact discretization of the normal derivatives of the viscous terms was used.

The model was placed in the identical heights above the ground as in the wind tunnel. This distance was measured from the upper boundary of the boundary layer momentum thickness of the ground plane to the reference point of the airfoil. Therefore the ground plane was simulated as inviscid wall (slip condition on the surface of the plane was used). This situation corresponded to the flying object over the stationary ground and it should be in agreement with the take-off or landing phase of the flight.

Calculations were performed as 2D, viscous, turbulent flow with k-ω SST two-equation model of turbulence. The turbulence model was chosen from previous experience of these kinds of computations and because of the expectation of separated regions on the airfoil and on the wall simulated the ground. K-ω turbulence model has better prediction of separation in comparison with other frequently used S-A model of turbulence.

6 Results

6.1 Experimental Results

6.1.1 Pressure distribution

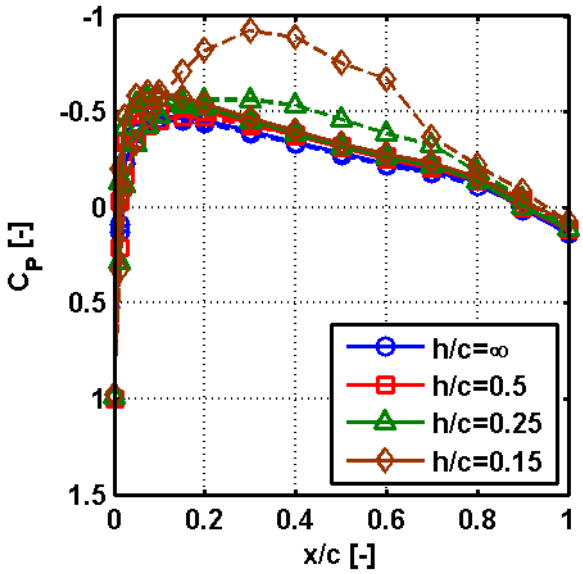

Fig. 1 Pressure distribution, α = 0 deg

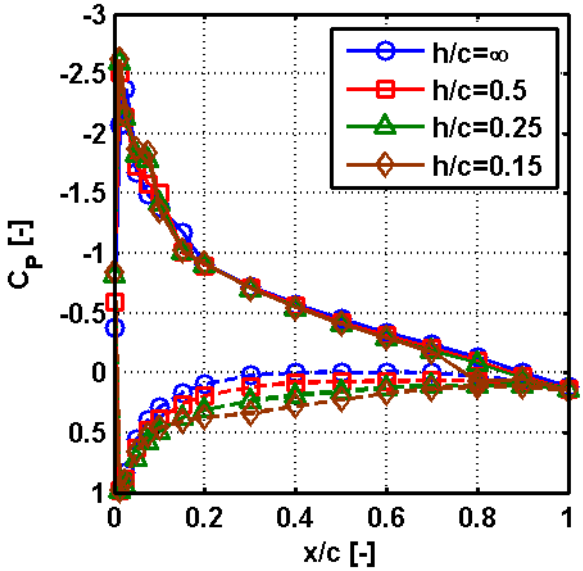

Fig. 2 Pressure distribution, α = +6 deg

The pressure distributions for the angles of attack of 0 deg and of +6 deg are presented in Fig. 1 and Fig. 2 respectively (note that the scales on the vertical axes are not identical); the distributions on the upper side of the airfoil are represented by solid lines, the distributions on

the lower side by dash lines. The aerodynamic asymmetry caused by the ground effect at $\alpha = 0$ is clearly distinguishable as the airfoil is geometrically symmetrical.

Upper side of airfoil

The modifications of the pressure distribution on the upper side of the airfoil are moderate. The all distributions feature similar shapes for all heights above the ground plane and their shapes are relatively similar to the distribution in the unrestricted space. The maximum differences are of the order of $\Delta C_p = 0.3$ at the position of 5 per cent of the airfoil chord.

Lower side of airfoil

The differences are evidently more pronounced than on the upper side. The distributions develop nonlinearly with the diminution of the height, from the typical shape of the pressure distribution of airfoil in unrestricted space to the shape typical rather for the flow in a nozzle (clearly visible for $h/c = 0.15$). Certain sensitivity on the angle of attack is also observed, for the negative angles of attack, the transition from the free space to the nozzle flow occurs for lower h/c then in the case of positive angles of attack. For example, for $\alpha = -2$ deg, the shape of the distribution of $h/c = 0.25$ differs clearly from the shape of $h/c \rightarrow \infty$. For $\alpha = +2$ deg, the shape of $h/c = 0.25$ is similar as of $h/c \rightarrow \infty$.

6.1.2 Lift

The lift curves for different h/c create a set in "fan form", the curves revolve round the "focus" at the angle of attack of 2 degrees (Fig. 3). The characteristics of the airfoil at the negative angles of attack are more influenced than for the positive angles. All principal lift curve characteristics are influenced by the changes of the height above the ground.

The difference of lift coefficient at $\alpha = 0$ changes in comparison with free space from $\Delta C_{L0} = +0.04$ to $\Delta C_{L0} = -0.19$. With the approaching of the airfoil to the ground plane, the C_{L0} initially slightly increases and then drops.

The lift curve slope at $\alpha = 0$ increases continuously with the reduction of the h/c. For $h/c = 0.15$, the slope is 1.85-times higher than for $h/c \rightarrow \infty$.

Maximum lift coefficient increases continuously with the diminution of the h/c, the increase by 17 per cent is registered between the free space and $h/c = 0.15$. For h/c lower than 0.75, the increase of the maximum lift coefficient is accompanied by the diminution of the angle of attack of the stall.

The stall behaviour is different for the different heights, the stall develops in more gentle manner for higher heights.

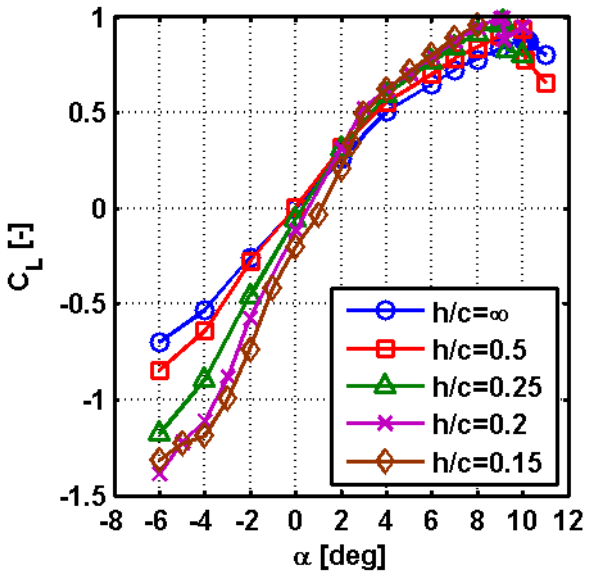

Fig. 3 Lift curves

6.1.3 Drag

The basic tendency with the diminution of h/c consists in the changes of general shape of the polar curve - the minimum drag decreases and the point of minimum drag shifts to the higher lift coefficients (Fig. 4).

The intensity of the influence of the height strongly depends on the angle of attack. The maximum reduction of $C_{D\,MIN}$ is observed for $\alpha = 4$ degrees, when $C_{D\,MIN}$ is reduced even by 50 per cent for $h/c = 0.20$, in comparison with the value for $h/c \rightarrow \infty$.

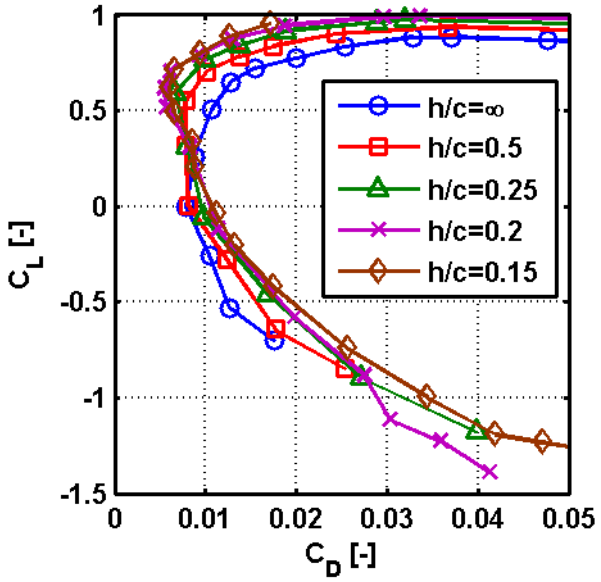

Fig. 4 Polar curves

As in the case of the lift, the values of drag at negative angles of attack are more influenced than at the positive ones.

6.1.4 Lift-to-drag ratio

The lift-to-drag ratio increases with the reduction of the height for positive lift coefficients (Fig. 5). On the contrary, for negative lift coefficients, the absolute value of the lift-to-drag ratio diminishes with the approach of the airfoil to the ground plane.

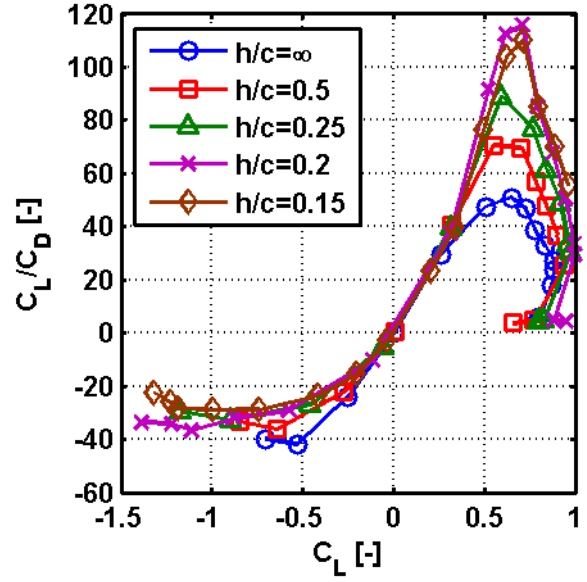

Fig. 5 Lift-to-drag ratio

6.1.5 Moment

The changes of the moment curve are low for h/c higher than 0.5, then the moment coefficient increases up to C_m = 0.05 with further height reduction (Fig. 6).

Position of the aerodynamic centre changes, the slight shift by maximally 2,5 percent of the chord towards the trailing edge is registered.

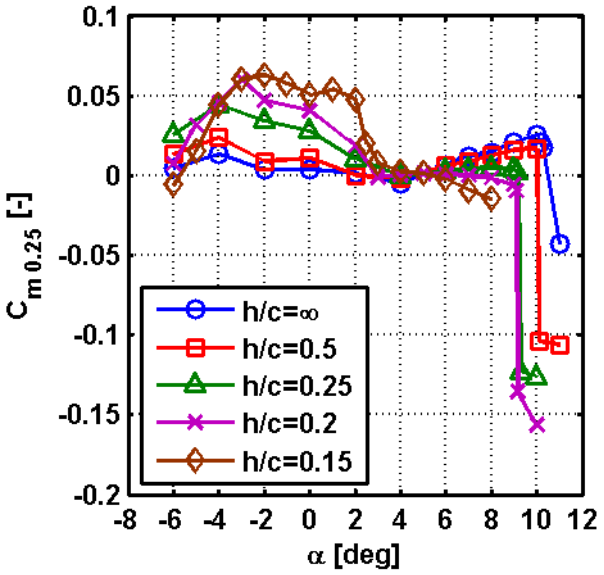

Fig. 6 Moment curves

6.2 Computational results

6.2.1 Comparison of different relative movements

The question rose about the practical usability of the wind tunnel results for the glider take-off analysis regarding the disproportion in the relativity of motions between the wind tunnel case with the fixed ground plane and the real flight case.

CFD computations were used to examine the aerodynamic differences caused by that disproportion. The results are presented in Fig. 7 and Fig. 8 where the velocities in the flow field for h/c = 0.25 (the warmer colour, the higher velocity) are visualized. The main difference in the flow fields is found on the ground below the airfoil section. In the wind tunnel case with the ground plate immobile with respect to the airfoil, a zone of the flow detachment is developed under the rear part of the airfoil for negative angles of attack and under the airfoil

leading edge for the positive angles of attack. Such detached zone is not observed in CFD results for the airfoil flying over the ground in a correct manner corresponding to real flight.

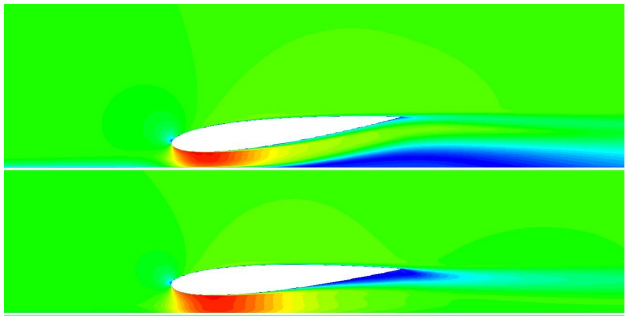

Fig. 7 Difference between viscous (upper part of the figure) and inviscid wall, negative α

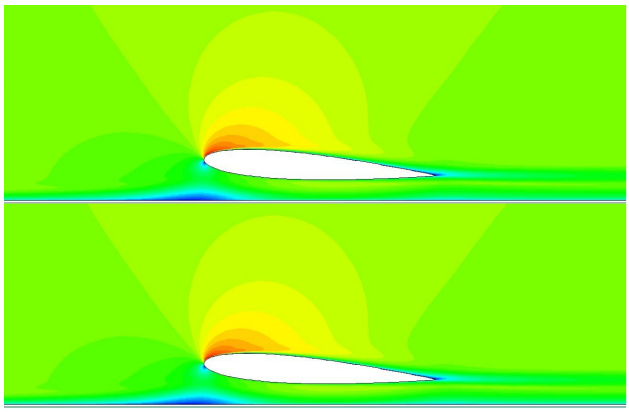

Fig. 8 Difference between viscous (upper part of the figure) and inviscid wall, positive α

For the practical use of the wind tunnel results, mainly the difference of the global aerodynamic characteristics seems to be important. The CFD shows the difference in lift curve slope in the order of few percent depending of the height over the ground (Fig. 9). An example of differences of C_L at a constant angle of attack at a constant height is presented in Fig 10, the difference is below 10 per cent even for extremely low height h/c = 0.15.

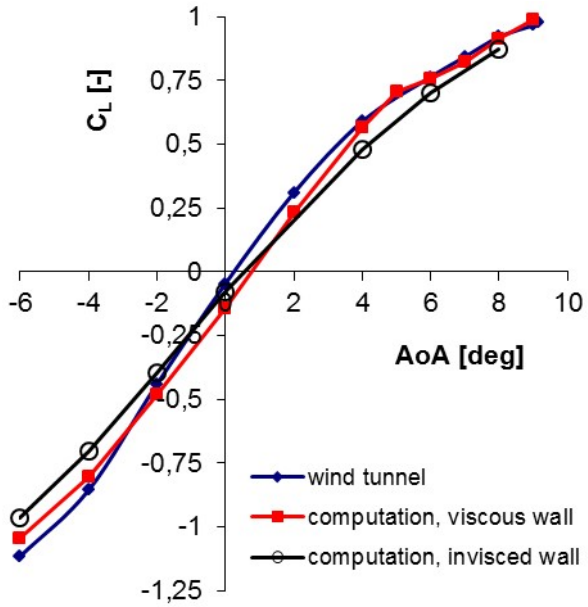

Fig. 9 Difference in lift curves, h/c=0.25

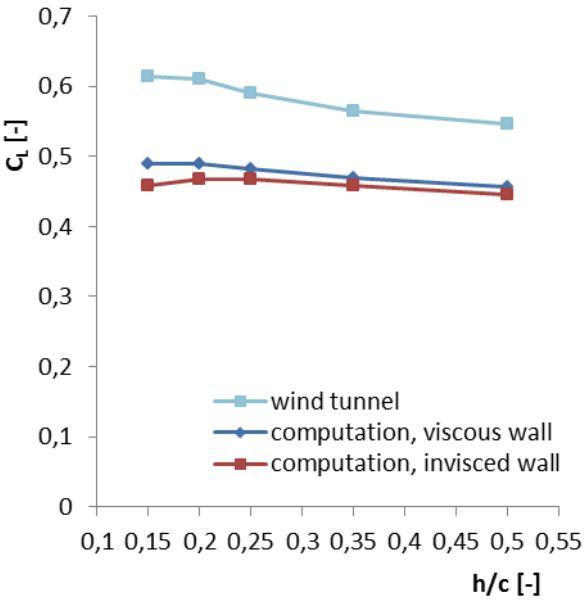

Fig. 10 Lift coefficient for α = +4deg

Based on the CFD computations, it is possible to conclude that the wind tunnel results are usable not only for understanding the fundamental principle of the phenomenon influencing the glider take-off but also to provide acceptable representation of the order of magnitude of the ground effect influence.

6.2.2 Pressure distribution

Pressure distributions obtained from calculation with the viscous wall were very close to the experimental results, the character of the

pressure distribution was well captured (Fig. 11 to Fig. 14). Note at the negative angles of attack that the lower curve in the graphs (with C_p in range from +1.0 to -0.2 or -0.3) belongs to the upper side of the airfoil.

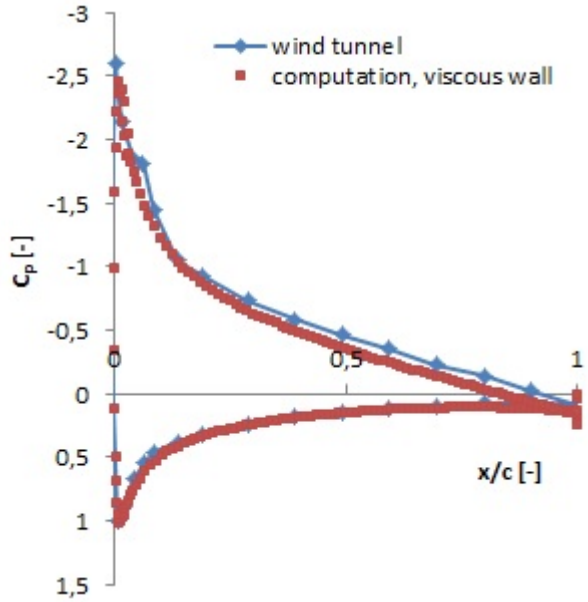

Fig. 11 Pressure distribution h/c=0.25, α = +6 deg

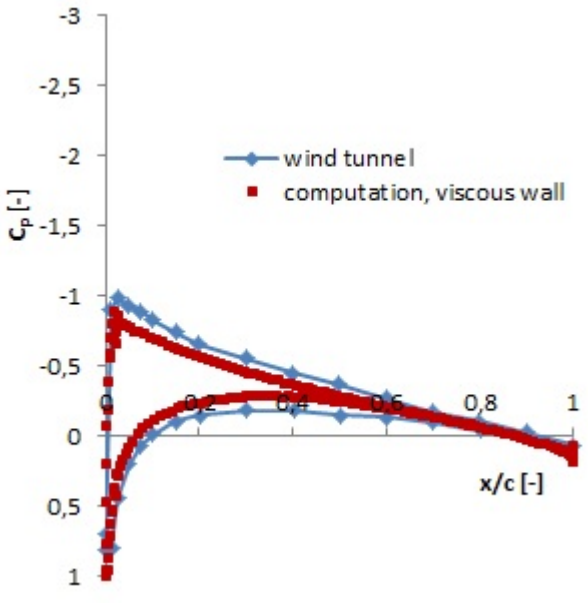

Fig. 12 Pressure distribution h/c=0.25, α = +2 deg

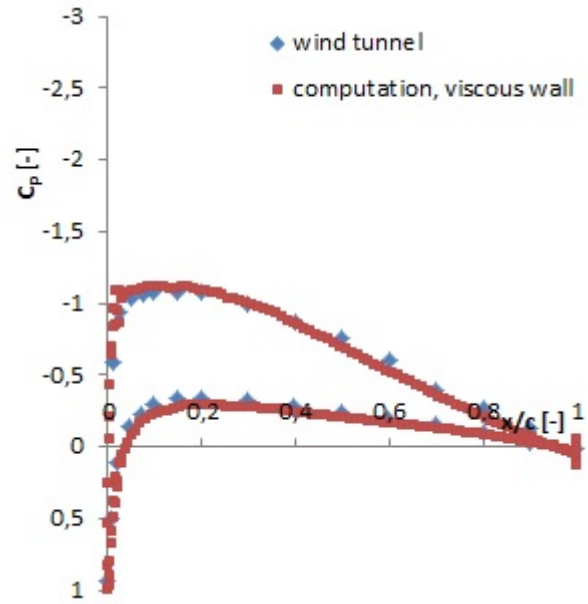

Fig. 13 Pressure distribution h/c=0.25, α = -2 deg

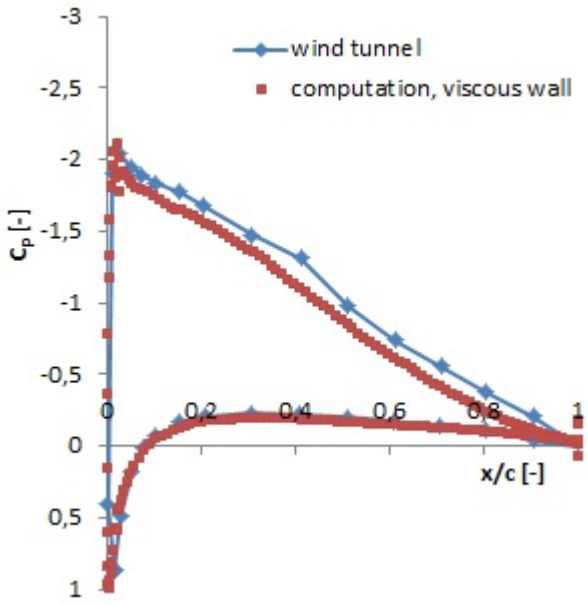

Fig. 14 Pressure distribution h/c=0.25, α = -4 deg

7 Conclusions

The ground effect depends essentially on the height above the ground, its pronouncement increases highly progressively as the airfoil approaches to the ground plane. The changes of the aerodynamic characteristics can reach very significant level, the lower surface of the airfoil is evidently much more influenced than its upper surface. The ground effect is pronounced

more for the negative angles of attack than for the positive angles. In certain cases of short distance between the airfoil and the ground plane, depending on the angle of attack, the transformation of the quality of the flow occurs, the flow physics changes from the external airfoil aerodynamics rather to the internal nozzle aerodynamics.

The results allow better understanding of the phenomena of the sailplane wing sticking to the ground. The sailplane undercarriage is generally designed with single main wheel so the bank of the plane accompanied by the approach of the wingtip to the ground is quite common during the initial stages of the take-off run, whether caused by the grass runway roughness, imperfections of the control or by side wind or gusts. The propagation of the troubles can be boosted by the low efficiency of aileron deflections at low speed which prevents pilot to take quick effective corrective action. The wingtip is designed with the washout in the most cases. Thus the two triggering conditions for the "adhesion" of the wingtip – low height above the ground and low angle of attack - can frequently occur. The flexibility of the wingtip of the most of glass or carbon fibre composite wings contributes to the bending and twist deformation of the extreme outer part of the wing and thus to its adhesion to the ground. Impossibility to elevate the wingtip together with the high friction and resistance of the higher grass can lead to the aforementioned failed take-off.

References

[1] Raymond A E. *Ground influence on airfoils*, NACA TN 67, 1921.

[2] Zerihan, J, Zhang X. Aerodynamics of a Single Element Wing in Ground Effect. *Journal of Aircraft*, Vol. 37, No. 6, pp. 1058 – 1064, 2000.

[3] Hsiun C M, Chen C K. Aerodynamic Characteristics of a Two-Dimensional Airfoil with Ground Effect. *Journal of Aircraft*, Vol. 33, No. 2, pp. 386 – 392, 1996.

[4] Couliette C, Plotkin A. Aerofoil Ground Effect Revisited, *The Aeronautical Journal*, Vol. 100, No. 992, pp. 65 – 74, 1996.

[5] Smith J L, Graham H Z, Smith J E. *The Validation of an Airfoil in the Ground Effect Regime Using 2-D CFD Analysis.* AIAA Paper 2008-4262.

[6] Ahmed M R, Sharma S D. An investigation on the aerodynamics of a symmetrical airfoil in ground effect. *Experimental Thermal and Fluid Science*. Vol. 29, No. 6, pp. 633-647, 2005.

[7] Ahmed M R, Takasaki T, Kohama Y. Aerodynamics of a NACA 4412 airfoil in ground effect, *AIAA Journal*, Vol. 45, No.°1, pp. 37-47, 2007.

[8] Ranzenbach R, Barlow J B. *Two-Dimensional Airfoil in Ground Effect, an Experimental and Computational Study*. Society of automotive engineers Paper 94-2509.

[9] Ranzenbach R, Barlow J B. *Cambered Airfoil in Ground Effect, an Experimental and Computational Study*. Society of automotive engineers Paper 96-0909.

[10] Barlow J B, Rae W H, Pope A. *Low-speed wind tunnel testing*. 3 edition, Wiley-Interscience, 1999.

[11] Eliasson P. EDGE, a Navier-Stokes Solver for Unstructured Grids, *Proc Finite Volume for Complex Applications III*, Porquerolles, ISBN 1 9039 9634 1, ISTE Ltd., London, pp 527-534, 2002.

8 Contact Author Email Address

patek@vzlu.cz

Copyright Statement